

# Relationship Between Growth Stress, Mechanical-Physical Properties and Proportion of Fibre with Gelatinous Layer in Chestnut (*Castanea Sativa* Mill.)

By Bruno Clair, Julien Ruelle and Bernard Thibaut

Laboratoire de Mécanique et Génie Civil, Équipe Bois, Université Montpellier 2, France

## Keywords

Growth stress  
Longitudinal Young's  
modulus  
Shrinkage  
Normal wood  
Tension wood  
Gelatinous layer  
*Castanea Sativa*

## Summary

A range of mechanical and physical properties were determined for 96 specimens of chestnut wood and for wood types ranging from compression to tension wood; tests included (1) growth stress, (2) longitudinal Young's modulus in green and air-dried states (3) shrinkage in longitudinal and tangential directions. Anatomical observations permitted determination of the proportion of fibres with a gelatinous layer. The influence of these atypical fibres on macroscopic wood properties is examined and discussed. A basic model is proposed to determine their properties in theoretically isolated conditions.

## Introduction

In angiosperms a high level of growth stress is associated with tension wood (Trénard and Guéneau 1975; Sassus 1998) which is usually positioned in the upward-facing half of leaning stems. In such stems, the distribution of growth stress measured at the periphery of the trunk is strongly heterogeneous. The upward-facing sector can have a tensile stress five times higher than normal values found elsewhere in the stem (Fournier *et al.* 1994; Sassus 1998). Sometimes very low values of tensile growth stress are measured on the part of the wood cylinder opposite the upward facing side. This heterogeneity in mechanical development can be so marked that by the end of the lignification process, portions of the new wood layer of a single tree can exhibit various levels of pre-stressing.

For many species such as beech, poplar, oak and chestnut, tension wood is characterised by the occurrence of fibres with a special morphology and chemical composition due to the development of the so-called gelatinous layer, which replaces the  $S_3$  layer and part of the  $S_2$  layer of the secondary wall (Onaka 1949). These cells, referred to hereafter as G fibres, are often abundant in tension wood, sometimes distributed randomly and sometimes in thin layers (Grzeskowiak *et al.* 1996; Jourez *et al.* 2001).

Although tension wood has been studied less than compression wood (Timell 1986), many studies have found that typical tension wood often has different properties from normal wood and, most notably, a higher longitudinal shrinkage (Chow 1946). Most observations have concerned homogeneous hardwoods such as beech or poplar and some studies have focused on the

relationship between local levels of growth stress and mechanical-physical properties of the wood situated at the same position (Baillères 1994; Combes *et al.* 1996; Grzeskowiak *et al.* 1996; Sassus 1998; Coutand *et al.* in press 2002). Among angiosperms studied, only beech and poplar show evidence of tension wood with G fibres. In both cases, large longitudinal maturation strains with high levels of tensile growth stress correspond to large longitudinal hygroscopic shrinkage. Only poplar appears to show evidence of significant variations in longitudinal Young's modulus, and this in very young shoots.

Chestnut (*Castanea Sativa* Mill.) hardwood consists of an initial ring porous zone, small uniseriate rays and very straight grain. Because of this organisation, it is of interest for testing properties in the longitudinal direction. Furthermore, tension wood in chestnut, although easily recognisable by its brown colour, is not mentioned as a drawback by users in industry and does not show signs of the “fuzzy grain” observed in poplar and beech.

In this paper we investigate the physical properties of chestnut wood with relation to G fibre content and discuss how this remarkable structure contributes to the macroscopic properties of wood.

## Materials and Methods

In France, timber from chestnut trees is mostly produced from small-diameter trees in coppiced forests. Two inclined trees of about 15 cm in diameter were selected in order to collect samples containing tension wood. Growth Stress Indicator (GSI) measurements were performed on the upper- and lower-facing halves of the trunk at several heights. The two trees were sam-

pled from 8 zones covering a wide range of GSI values (Fig. 1, underlined values).

Sample dimensions ( $1 \times 5 \times 50$ – $75$  mm) were optimised so as to record measurements from locations on the stem as precisely as possible and to permit measurement of the physical and mechanical properties in the axial direction. All samples were prepared with a band saw equipped with a motorised guide permitting sawn veneers from 1 to 1.5 mm thick. Three veneers were taken successively from the vicinity of each GSI measurement hole and cut into 4 samples of  $5 \times 70$  mm on a circular mini-saw, during which a precise orientation of the specimen with respect to wood anisotropy was maintained. We thus obtained 12 samples for each GSI value (Fig. 2). The entire study constituted 96 samples distributed around 8 known GSI values. Samples were stored in water from their extraction in field conditions to the end of machining.

#### Growth Stress Indicator (GSI)

The “single hole” drilling method developed by Cirad (Fournier *et al.* 1994) was used to estimate the longitudinal growth stress on both the upper- and lower-facing surfaces of the leaning tree at every sampled height. This method gives the value of the displacement between two pins, hammered onto the trunk (after local debarking) at a 45 mm distance from each other. A hole (20 mm depth and 20 mm diameter) is drilled at the mid-point between the two pins. The value in  $\mu\text{m}$  is termed the Growth Stress Indicator (GSI) and is directly proportional to longitudinal growth stress at the trunk periphery with a relationship slightly dependant on the mechanical anisotropy of the species. As such, values of GSI are good indicators of relative growth stresses within trees of the same species.

The results of the GSI measurements are given in Figure 1. GSI values vary from  $-10$  (low value = compression wood) to  $+135$   $\mu\text{m}$  (around 3 times the mean value for normal wood in tension). Surprisingly, compression values as small as found here ( $-10$   $\mu\text{m}$  compared to  $-100$   $\mu\text{m}$  for typical compression wood in pine) are seldom found in hardwood trees except for Box (*Buxus sempervirens*) (Baillères *et al.* 1997). In the case of chestnut, a database of values representing 1206 measurements from 150 trees using the same method gives values distributed evenly from  $-10$  to  $+360$   $\mu\text{m}$  (Thibaut *et al.* 1995). Until now, it has not been clear whether such values were artefactual or resulted from local differences in wood mechanical behaviour.

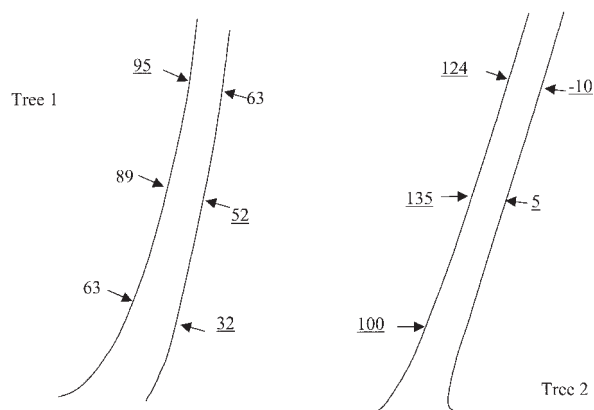


**Fig. 1.** GSI measurement values on upper- and lower-facing sides of two inclined chestnut trees at several heights; underlined values indicate those chosen for the study.

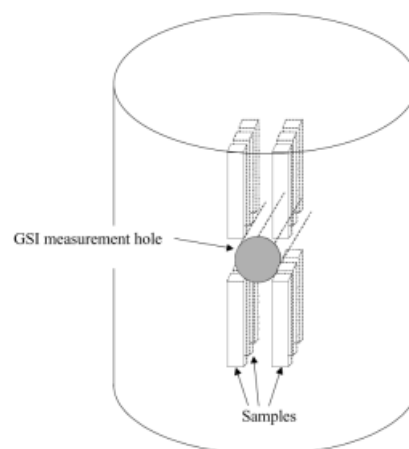


**Fig. 2.** Cutting protocol for samples, showing position and depth within the stem of 3 original veneers, each cut into 4 separate veneer segments.

#### Basic density

Sample mass was measured with a Sartorius balance (precision 0.001 g). Volumes were measured by the convenient double weight method (Archimedes principle) in which the sample is first weighed in air and then a second time immersed in water. The force resulting from immersing the sample in water is measured as the difference in mass. The volume is then determined as:  $\text{Volume} = (M_a - M_w) / \rho_w$ , with  $M_a$  the mass of the sample in air,  $M_w$  the mass of the sample in water and  $\rho_w$  the density of water at the working temperature.

Basic density values are between 0.32 and 0.60  $\text{g}/\text{cm}^3$  with a mean value of 0.45  $\text{g}/\text{cm}^3$  and a standard deviation of 0.054. Samples of very low density come from a very weak growth zone characterised by mostly porous wood growth and little fibre development and those of high density from a strong growth zone where there is production of fibres with a gelatinous layer.

#### Longitudinal Young's Modulus

Tests were performed both under water saturated and air-dry conditions on a mechanical testing machine (DARTEC). Tests were carried out in tension parallel to fibres with a load cell of 25 kN capacity. An extensometer measured the displacement between two “knives”, which are clamped onto the wood specimen in a central position with regard to the two holders anchoring the test piece. The global error with this type of measurement is less than 3%. The elastic moduli are strongly related to the sample density; we also present the specific moduli, which are calculated as the ratio of the modulus to the basic density (BD) of the sample (Table 1).

#### Shrinkage

Shrinkage was calculated as the ratio of the dimensional variation between saturated and dried states on the dimension in the saturated state. Tangential and longitudinal dimensions were measured relative to a reference. The measurement device was made up of two transducers (Mitutoyo type) linked to a sample positioning system (Fig. 3). The dried state was obtained by oven drying at  $103^\circ\text{C}$  for 2 days. Results of shrinkage measurements are given in Table 2.

#### Anatomy and image analysis

After tension tests under water saturated conditions, both ends

of samples were used to make anatomical microtome sections (15  $\mu\text{m}$  in thickness), avoiding areas of tissue damaged by the experimental procedures.

Staining with both safranin + blue astra and Azur II was used to identify tension wood. Typical G layers were recognisable by their morphology and difference in colour as compared with other cell wall layers. Azur II was preferred for image analysis techniques, because the secondary wall is stained light blue and the gelatinous layer dark blue. Thus, "blue levels" can be digitised as grey levels without loss of information for further image analysis (Fig. 4).

Sections were observed with a compound microscope (Leica) and at a magnification of 50 $\times$ . Two images were taken of each sample in order to cover the whole surface of  $5 \times 1$  mm. Image capture was performed by means of a digital camera (1316  $\times$  1034 pixels in 256 grey levels) and the image analysis was done by the software Optimas (v.6.5). A threshold was used in order to separate woody material and cell lumens. This threshold was determined for each image by an automatic search of pixels at minimum grey levels. Contours of bands of cells with G layers were achieved manually for each image. For every anatomical section, the surface occupied by the woody

matter (WM) and surface of band of cells with G layer was extracted. A correction was performed on the diameter of every lumen to minimise the gap of density between macroscopic measurements and results according to the woody matter density on the anatomical cuts.

Quantity of fibres with gelatinous layer (noted GF) are expressed as percentages of the total surface of the cut (%GF/tot) and as percentage of the woody matter (total surface less the surface of the lumens: %GF/WM). The macroscopic properties were compared with reference to the quantities of fibres with a G layer, both for all the samples and for samples containing GF (noted NE). For each sample, the results correspond to the mean values measured at the two extremities.

According to the sampling, half of the tested samples include tension wood with a G layer and all proportion classes of G layer fibre are represented up to samples with 93 % woody matter.

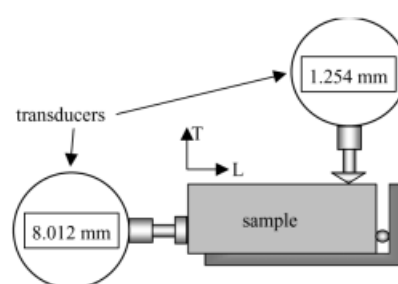


**Fig. 3.** Apparatus for measuring dimension changes of samples.

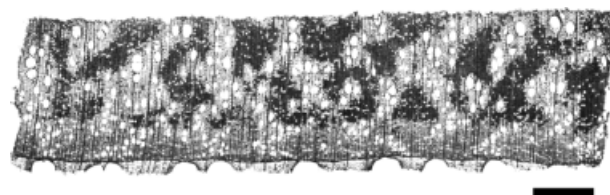


**Fig. 4.** Azur II staining of chestnut tension wood. Dark zones are fibres with gelatinous layer (scale bar = 500  $\mu\text{m}$ ).

**Table 1.** Statistical data on longitudinal Young's modulus of elasticity  $E$  (MPa) and specific modulus  $E/\text{BD}$  ( $\text{MPa} \cdot \text{cm}^3 \cdot \text{g}^{-1}$ ) under saturated and dry conditions. BD = basic density

	$E_{\text{sat}}$	$E_{\text{sat}}/\text{BD}$	$E_{\text{dry}}$	$E_{\text{dry}}/\text{BD}$
min	2300	5400	2300	5800
mean	7500	16200	10000	21400
max	19200	32600	30400	60700
SD	3200	5900	5200	9900

**Table 2.** Statistical data on shrinkage in longitudinal (L) and tangential (T) directions

	min	mean	max	SD
L	0.04 %	0.44 %	1.37 %	0.26 %
T	4.14 %	8.76 %	16.13 %	2.19 %

**Table 3.** Correlations between parameters.  $r$  values are given in the lower left half of the matrix and significance values in the upper right

	GSI	Infra density	shrink-age T	shrink-age L	Esat	Esat/BD	Edry	Edry/BD	%GF/tot	%GF/WM	%GF/tot (NE)	%GF/WM (NE)
GSI	1	NS	***	***	***	***	***	***	***	***	***	**
infradensity	0.1132	1	NS	*	NS	NS	NS	NS	NS	NS	NS	NS
shrinkage T	0.6062	0.1172	1	***	***	***	***	**	***	***	NS	NS
shrinkage L	0.7271	0.2091	0.4342	1	*	NS	**	**	***	***	**	***
Esat	0.4971	-0.0473	0.4954	0.2228	1	***	***	***	***	***	***	***
Esat/BD	0.4126	-0.1487	0.4103	0.0145	0.9486	1	***	***	***	***	**	**
Edry	0.4232	0.1147	0.3655	0.2849	0.6516	0.5867	1	***	***	***	***	***
Edry/BD	0.3812	0.0845	0.2972	0.3183	0.6231	0.5581	0.9639	1	***	***	***	***
%GF/tot	0.7541	0.1705	0.4863	0.7266	0.5688	0.3933	0.6339	0.6261	1	***	***	***
%GF/WM	0.8021	0.1791	0.5041	0.7401	0.5444	0.3733	0.6033	0.5839	0.9834	1	***	***
%GF/tot (NE)	0.4231	0.0047	0.1601	0.4124	0.5434	0.4468	0.6674	0.6941	1.0000	0.9705	1	***
%GF/WM (NE)	0.3993	-0.0105	0.1372	0.3682	0.5135	0.4267	0.6491	0.6623	0.9705	1.0000	0.9705	1

NS = non significant, \* = threshold less than 5 %, \*\* = less than 1 %, \*\*\* = less than 0.1 %.

## Results and Discussion

The correlation coefficients between the different properties are presented in Table 3. There are significant correlations between Growth Stress Indicator (GSI) and all parameters except basic density.

### GSI – % fibres with G layer

GF never occurred where the GSI was lower than 60 (normal wood) and was always present for GSI over 90 (tension wood) (Table 4). The sampling did not allow us to determine precisely the limit between normal and tension wood. The large variability of %GF for each GSI level can be explained by a variable content of normal wood and tension wood. GSI is a global value which is affected by a combination of all the areas of tension wood and normal wood in the vicinity of the GSI aperture drilled for the experiment. The 12 samples measured for mechanical-physical properties for each GSI measurement should therefore sample and reflect the variation in areas of tension and normal wood in the vicinity of the test.

### GSI – Shrinkage

Tangential shrinkage is linked to GSI (Fig. 5) in a single positive linear relationship. In longitudinal shrinkage, normal wood (GSI from –10 to 52  $\mu\text{m}$ ) and tension wood (GSI from 95 to 135  $\mu\text{m}$ ) can be separated (Fig. 6). Longitudinal shrinkage of normal wood decreases linearly with GSI, while the reverse is true for tension wood, as was previously found for other species such as poplar and beech (Sassus 1998). Both decreases in L shrinkage and increases in T shrinkage with an increase in GSI for normal wood without a G layer are similar to what is observed among conifers between compression wood and normal wood (Meylan 1972; Yamamoto *et al.* 1995; Sassus 1998). This observation is supported by the negative interrelationship between the tangential and longitudinal shrinkage, which would confirm that the same phenomenon inversely governs the two types of shrinkage (Fig. 7). For conifers, microfibril angle variations are considered the key factor (Meylan 1972). This

**Table 4.** Relation between GSI and proportion of fibre with G layer

GSI ( $\mu\text{m}$ )	% of GF (%)	
	Mean	CV
–10	0	0
5	0	0
32	0	0
52	0	0
95	14.2	7.2
100	25.7	11.3
124	27.0	16.4
135	35.8	19.7

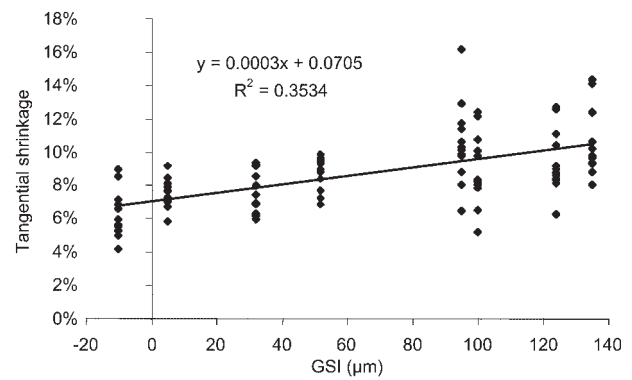


**Fig. 5.** Relation between tangential shrinkage and GSI.

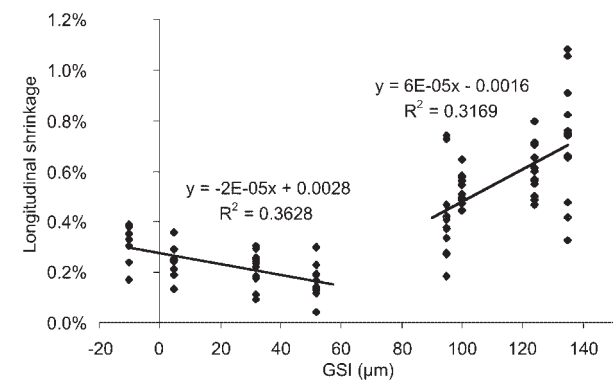


**Fig. 6.** Disjunct relation between longitudinal shrinkage and GSI

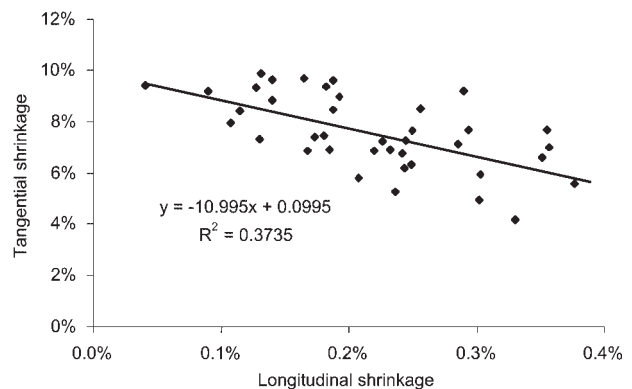


**Fig. 7.** Relation between longitudinal and tangential shrinkage for samples without G layer fibres.

should be examined further in normal wood of angiosperms such as chestnut.

The strong increase in longitudinal shrinkage with an increase in GSI in samples including some fibres with a gelatinous layer cannot be attributed to effects of the microfibril angle, because in gelatinous layers the microfibril angle is zero or very weak (Fujita *et al.* 1974). High longitudinal shrinkage was measured in beech and poplar tension wood (Clarke 1937; Chow 1946; Sassus 1998; Coutand *et al.* in press 2002). Boyd (1977) and Norberg and Meier (1966) hypothesise that L shrinkage



is due to an  $S_1$  layer that is generally thicker in tension wood and in which microfibril angle is more important. However, a study on G layer shrinkage showed that the strong shrinkage of the G layer can be the motor of this type of strong macroscopic shrinkage (Clair and Thibaut 2001).

#### GSI – Longitudinal Young's modulus

A positive linear relationship was found between longitudinal Young's modulus and GSI (Fig. 8). This observation has also been made on poplar (Coutand *et al.* in press 2002). However, other authors do not find any relation between these two measures or between longitudinal Young's modulus and the percentage of G fibres correlated with GSI (Chow 1946; Ferrand 1982a, b; Sassus 1998 on beech; Baillères 1994, on eucalyptus without G fibres; Sassus 1998, on poplar).

In beech, in terms of the behaviour of green state normal wood alone (GSI from  $-10$  to  $52 \mu\text{m}$ ), there is a strong relationship between GSI and longitudinal Young's modulus (Fig. 8). This could be explained, similar to longitudinal shrinkage, by variation in the microfibril angle in the  $S_2$  layer, as has been observed and modelled for softwoods (Cave 1969; Salmén and de Ruvo 1985; Koponen *et al.* 1989). In dry conditions, this relationship is weaker. It is possible that dehydration of small specimens can produce internal cracks, thus locally weakening samples of normal wood.

In tension wood samples there is a strong scattering of specific longitudinal Young's moduli, which is even more marked in the dry state. This can be partly explained by the same arguments as for L shrinkage: the 12 specimens used for longitudinal Young's modulus measurements at each GSI local hole position may represent differing strips and samples of tension wood and normal wood. In the dry state, micro cracks and delamination of the G layer during drying could be another reason for low values of longitudinal Young's modulus among tension wood specimens.

#### Role of G layer fibres in tension wood

There are high correlations between the two percentages of fibres with G layers (%GF/tot and %GF/WM) so only the first will be considered in the following discussion.

#### % fibres with G layer – shrinkage

There is a significant positive linear relationship between longitudinal shrinkage and percentage of G fibres (Fig. 9). This agrees well with results on L shrinkage within the G layer itself (Clair and Thibaut 2001). The correlation between tangential shrinkage and percentage of fibres, on the contrary, is not significant, although the G layer itself exhibits high transverse shrinkage that nevertheless does not seem to affect macroscopic shrinkage in the R or T direction.

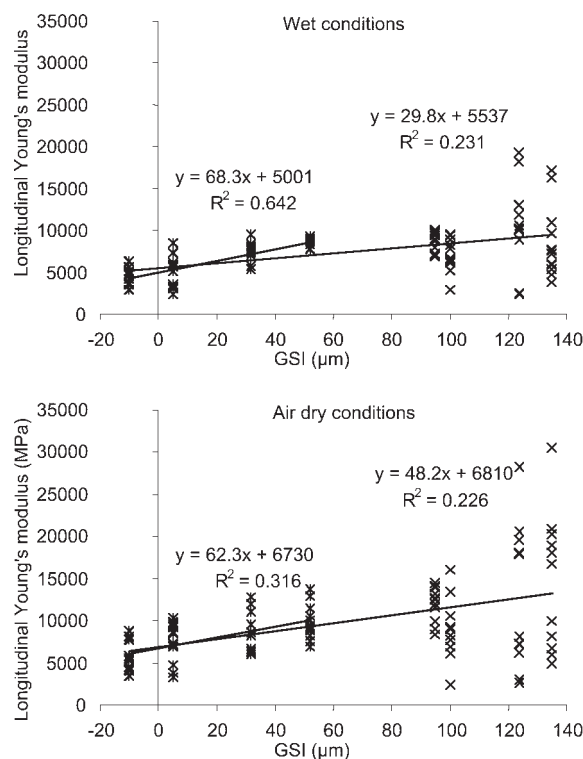


**Fig. 8.** Relation between longitudinal Young's modulus and GSI. Saturated and air-dry states. x: all GSI ; \*: GSI <  $60 \mu\text{m}$ .

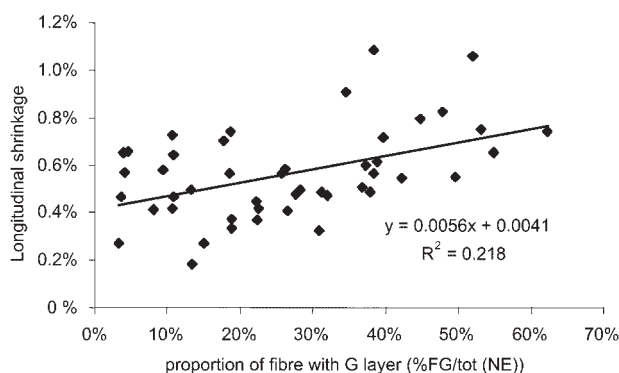


**Fig. 9.** Relation between longitudinal shrinkage and proportion of fibres with a G layer.

#### % fibres with G layer – elastic modulus

Under both saturated and air-dried conditions, longitudinal Young's modulus has a significant positive correlation with percentage of G fibres (Fig. 10), but this percentage explains only 20 to 30% of the variation in longitudinal Young's modulus. Variations are higher and correlation is more significant for the dry state than for the saturated state.

#### Identification of longitudinal Young's modulus and longitudinal shrinkage for both type of fibres.

A simple model can be built for investigating contributions to longitudinal properties considering the parallel

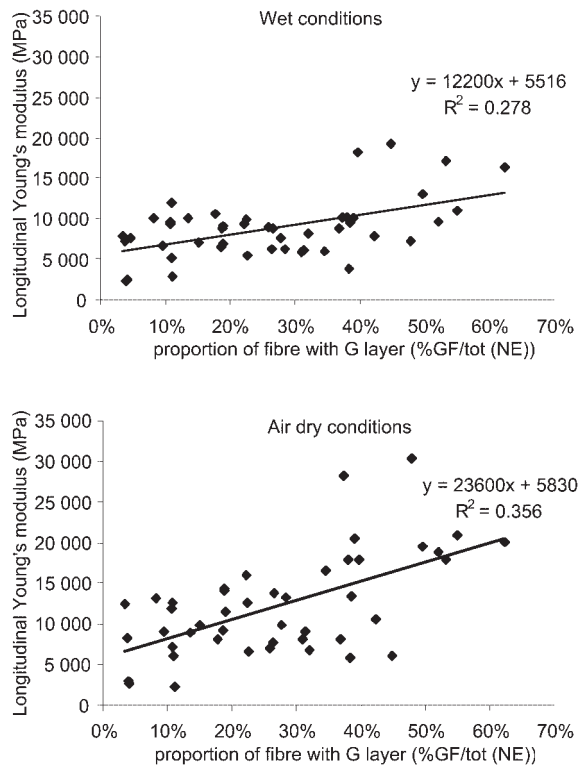


**Fig. 10.** Relation between longitudinal Young's modulus and proportion of fibres with a G layer. Saturated and air-dry states.

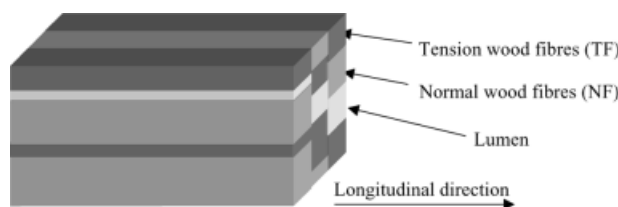


**Fig. 11.** Schematic representation of sample containing 2 different tissues and holes.

bundles of areas of normal wood fibres (NF), areas of tension wood fibres (TF) (fibres containing gelatinous layer) and empty areas (lumens of fibres and vessels) as described in Figure 11.

If a force (in the longitudinal direction)  $F_{\text{macro}}$  is applied on the surface of the sample  $S_{\text{macro}}$ , mean stress is given by

$$\sigma_{\text{macro}} = F_{\text{macro}} / S_{\text{macro}}$$

But longitudinal stress is not homogeneous across the whole RT surface of the sample and total force (macro) is equal to the sum of component forces. Total strain of the sample is supposed to be homogeneous, so strains of constituents are equal to the macroscopic strains.

$$\begin{aligned} \epsilon_{\text{TW}} &= \epsilon_{\text{NW}} = \epsilon_{\text{macro}} \\ F_{\text{macro}} &= \sigma_{\text{macro}} \cdot S_{\text{macro}} = \sigma_{\text{TF}} \cdot S_{\text{TF}} + \sigma_{\text{NF}} \cdot S_{\text{NF}} \\ \sigma_{\text{macro}} &= \sigma_{\text{TF}} \cdot S_{\text{TF}} / S_{\text{macro}} + \sigma_{\text{NF}} \cdot S_{\text{NF}} / S_{\text{macro}} \\ \sigma_{\text{macro}} &= \sigma_{\text{TF}} \cdot x_{\text{TF}} + \sigma_{\text{NF}} \cdot x_{\text{NF}} \end{aligned}$$

The elastic behaviour law is given by  $\sigma = E_L \cdot \epsilon$  where  $E_L$  is the longitudinal modulus of elasticity. Thus, macroscopic longitudinal Young's modulus is related to normal and tension fibre moduli by:

$$E_{\text{Lmacro}} = x_{\text{TF}} \cdot E_{\text{LTF}} + x_{\text{NF}} \cdot E_{\text{LNF}}$$

with  $x_{\text{TF}}$  and  $x_{\text{NF}}$ , respectively, representing the proportions of fibres with and without G layer respective to the total surface.

$E_{\text{LTF}}$  and  $E_{\text{LNF}}$  are assumed to be always the same in all specimens and are calculated by a least square optimisation on the experimental values of  $E_{\text{Lmacro}}$ ,  $x_{\text{TF}}$  and  $x_{\text{NF}}$  for the 48 specimens considered as tension wood (GSI > 80  $\mu\text{m}$ ). In the saturated state,  $E_{\text{LNF}} = 14500$  MPa and  $E_{\text{LTF}} = 21600$  MPa. In the air-dry state,  $E_{\text{LNF}} = 15100$  MPa and  $E_{\text{LTF}} = 31300$  MPa. There is a greater increase in rigidity between the saturated and air-dry states for cells with the G layer than for cells without the G layer. This would lead to a hypothesis of a stronger stiffening of the gelatinous layer during drying.

In order to estimate the longitudinal shrinkage of the fibres with and without G layers, the same type of approach can be used to calculate the force that should be necessary to prevent the strain from producing shrinkage. This force can be written as the product of the longitudinal Young's modulus, shrinkage and concerned surfaces, leading to the following equation:

$$E_{\text{Lmacro}} \cdot \alpha_{\text{Lmacro}} = x_{\text{TF}} \cdot E_{\text{LTF}} \cdot \alpha_{\text{TF}} + x_{\text{NF}} \cdot E_{\text{LNF}} \cdot \alpha_{\text{NF}}$$

Values of  $\alpha_{\text{LTF}}$  and  $\alpha_{\text{LNF}}$  are also adjusted by looking for a minimum for the sum of the squares of the differences between experimental and theoretical values. Using longitudinal Young's modulus under saturated conditions,  $\alpha_{\text{NF}} = 0.34\%$  and  $\alpha_{\text{TF}} = 0.71\%$ . Using longitudinal Young's modulus under air-dry conditions,  $\alpha_{\text{NF}} = 0.29\%$  and  $\alpha_{\text{TF}} = 0.69\%$ .

The difference in L shrinkage between fibres with and without the G layer is rather weak and the value for normal fibres is a little higher than the mean value for macroscopic L shrinkage of normal wood (although it is in the range of the values obtained).

According to the literature, axial shrinkage of tension wood is often more than 5 times higher than that of normal wood for beech or poplar (Sassus, 1998). On the one hand, severe tension wood can be associated with GSI values higher than those considered in this experiment, more than 300  $\mu\text{m}$  for chestnut for example (Fournier *et al.* 1994). On the other hand, chestnut tension wood is not considered as a big problem for industrial applications. The small differences observed here between normal and tension wood might be specific to chestnut wood and this should be assessed from more specimens and more trees.

## Conclusions

This study shows meaningful relationships between growth stress and mechanical and physical properties in normal wood, especially in the longitudinal direction. In

the absence of fibres with a gelatinous layer, variations of longitudinal Young's modulus and shrinkage in L and T directions concur with a model of the cell wall governed by variations of the microfibril angle in the S<sub>2</sub> layer. This should be studied in the case of chestnut on a large scale of GSI values with both careful measurements of material properties and MFA.

It is not known whether the difference in GSI for tension wood (between around 90 µm to more than 300 µm) is only due to the percentage of G layer fibres, and/or to the "properties" of these G layer fibres. Furthermore, the difference in L shrinkage in tension wood that seems to exist between different species such as beech or poplar on one hand and chestnut (and maybe oak) on the other should be related to some structural parameters such as organisation of crystalline zones in G layer (?) or chemical composition of the cell wall components. This should be investigated in the future on more species, and more specimens per species.

### Acknowledgements

We thank Nick Rowe for checking the English and making improvements to the manuscript.

### References

- Baillères, H. 1994. Précontraintes de croissance et propriétés mécano-physiques de clones d'Eucalyptus (Pointe-Noire, Congo): Hétérogénéités, corrélations et interprétations histologiques. PhD Thesis. Université Bordeaux I. 161 pp.
- Baillères, H., M. Castan, B. Monties, B. Paullet and C. Lapierre. 1997. Lignin structure in *Buxus sempervirens* L. reaction wood. *Phytochemistry* 44(1), 35–39.
- Boyd, J.D. 1977. Relationship between fibre morphology and shrinkage of wood. *Wood Sci. Technol.* 11, 3–22.
- Cave, I.D. 1969. The longitudinal Young's modulus of *Pinus radiata*. *Wood Sci. Technol.* 3, 40–48.
- Chow, K.Y. 1946. A comparative study of the structure and composition of tension wood in beech (*Fagus sylvatica* L.). *Forestry* 20, 62–77.
- Clair, B. and B. Thibaut. 2001. Shrinkage of the gelatinous layer of poplar and beech tension wood. *IAWA J.* 22(2), 121–131.
- Clarke, S.H. 1937. The distribution, structure and properties of tension wood in beech (*Fagus sylvatica* L.). *J. For.* 11(2), 85–91.
- Combes, J.G., F. Sassus, H. Baillères, B. Chanson and M. Fournier. 1996. Les bois de réaction: Relation entre la déformation longitudinale de maturation et les principales caractéristiques physico-mécaniques, anatomiques et chimiques. In: 4ème Colloque Sciences et Industries du Bois. Ed. Haluk. ARBOLOR, Nancy. pp. 75–82.
- Coutand, C., G. Jeronimidis, B. Chanson and C. Loup. in press 2002. Comparison of mechanical properties of tension and normal wood in *Populus*. *Wood Sci. Technol.*
- Ferrand, J.C. 1982a. Etude des contraintes de croissance. I: Méthode de mesure sur carottes de sondage. *Ann. Sci. For.* 39(2), 109–142.
- Ferrand, J.C. 1982b. Etude des contraintes de croissance. II: Variabilité en forêt des contraintes de croissance du Hêtre (*Fagus sylvatica* L.). *Ann. Sci. For.* 39(3), 187–218.
- Fournier, M., B. Chanson, B. Thibaut and D. Guitard. 1994. Mesure des déformations résiduelles de croissance à la surface des arbres, en relation avec leur morphologie. Observation sur différentes espèces. *Ann. Sci. For.* 51(3), 249–266.
- Fujita, M., H. Saiki and H. Harada. 1974. Electron microscopy of microtubules and cellulose microfibrils in secondary wall formation of poplar tension wood fibers. *Mokuzai Gakkaishi* 20(4), 147–156.
- Grzeskowiak, V., F. Sassus and M. Fournier. 1996. Coloration macroscopique, retraits longitudinaux de maturation et de séchage du bois de tension du Peuplier (*Populus x euramericana* cv. I.214.). *Ann. Sci. For.* 53(6), 1083–1097.
- Jourez, B., A. Riboux and A. Leclercq. 2001. Anatomical characteristics of tension wood and opposite wood in young inclined stems of poplar (*Populus euramericana* cv "ghoy"). *IAWA J.* 22(2), 133–157.
- Koponen, S., T. Toratti and P. Kanerva. 1989. Modelling longitudinal elastic and shrinkage properties of wood. *Wood Sci. Technol.* 23, 55–63.
- Meylan, B.A. 1972. The influence of microfibril angle on the longitudinal shrinkage – moisture content relationship. *Wood Sci. Technol.* 6(4), 293–301.
- Norberg, P.H. and H. Meier. 1966. Physical and chemical properties of the gelatinous layer in tension wood fibre of aspen (*Populus tremula* L.). *Holzforschung* 20, 174–178.
- Onaka, F. 1949. Studies on compression and tension wood. Wood research, Bull. Wood Research Institute, Kyoto University, Japan 24(3), 1–88.
- Salmén, L. and A. de Ruvo. 1985. A model for the prediction of fiber elasticity. *Wood Fiber Sci.* 17(3), 336–350.
- Sassus, F. 1998. Déformations de maturation et propriétés du bois de tension chez le hêtre et le peuplier: Mesures et modèles. PhD Thesis. ENGREF, Montpellier.
- Thibaut, B., B. Chanson, M. Fournier and D. Jullien. 1995. Valorisation du bois de châtaignier: Prévoir et réduire les risques de roulure à la production. Rapport final contrat "Agriculture Demain" MRT 91.G.0491.
- Timell, T.E. 1986. Compression Wood in Gymnosperms. Springer Verlag, Berlin.
- Trénard, Y. and P. Guéneau. 1975. Relations entre contraintes de croissance longitudinales et bois de tension dans le hêtre (*Fagus sylvatica* L.). *Holzforschung* 29 (6), 217–223.
- Yamamoto, H., T. Okuyama and M. Yoshida. 1995. Generation process of growth stresses in cell walls IV: Analysis of growth stress generation using a cell model having three layers (S1, S2 and I+P). *Mokuzai Gakkaishi* 41(1), 1–8.

Received December 19<sup>th</sup> 2001

Bruno Clair<sup>1)</sup>  
Julien Ruelle  
Bernard Thibaut  
Laboratoire de Mécanique et Génie Civil  
Equipe Bois, CC 081  
Université Montpellier 2  
Place Eugène Bataillon  
34095 Montpellier Cedex 5  
France

<sup>1)</sup> Corresponding Author.  
Email: clair@lmgc.univ-montp2.fr